Electronic Supplementary Material (ESI) for New Journal of Chemistry.

Supplementary data

Silanated nano ZnO hybrids embedded PMMA polymer coatings on cotton fabrics for near-IR reflective, antifungal cool-textiles

S. Soumya,[a] S. Nishanth Kumar,[b] A. Peer Mohamed,[a] and S. Ananthakumar*[a]

[a]*Functional Materials Section, Materials Science and Technology Division,*

[b]*Agro processing and Natural Products Division,*

Council of Scientific and Industrial Research-National Institute for Interdisciplinary Science and Technology (CSIR-NIIST), Thiruvananthapuram-695019, Kerala, India

Corresponding author: *ananthakumar70@gmail.com, Tel: 91-471-2515289 or 91-9497271547 Fax: 91-471-2491712

Effect of silane treatment on the bulk properties of ZnO nanohybrids.

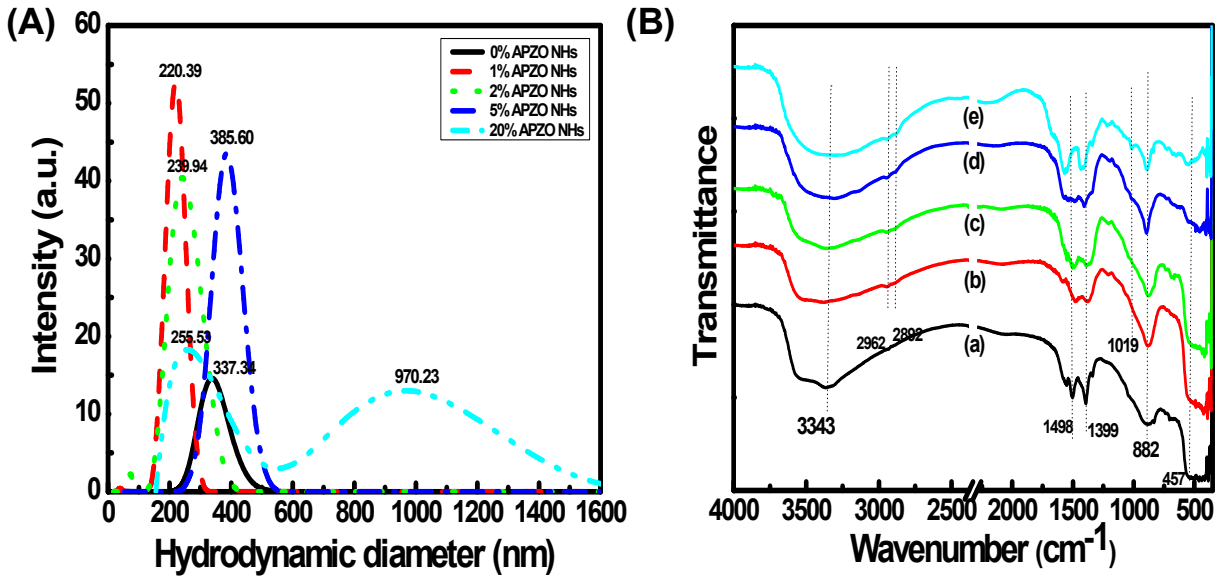

Fig. S1. (A) DLS Particle size distribution analysis of APZO NHs with respect to silane modification (a) 0, (b) 1, (c) 2, (d) 5, and (e) 20% APZO NHs. (B) FTIR spectra of unmodified and different concentration of APZO NHs.

Fig. S1B shows the FTIR spectra of ZnO hybrids prepared with 1 mol.% of silane. In FTIR spectra, the broad peak existing between the wavelengths ~3262-3540 cm^{-1} represents the –OH stretching. The chemical adsorption of the water molecules generates the hydroxyl groups onto the ZnO particle surface through hydrogen bonding. The two broad bands in the wavelength region ~ 457- 427 cm^{-1} clearly indicate the Zn-O bonding. Upon silane treatment, in the APZO NHs asymmetric and symmetric stretching modes of $–CH_2$ groups appeared at wavelength ~2962 and ~2892 cm^{-1}. A vibrational mode typical of ammoniumpropyl moieties is also observed in the wavelengths 1600-1400 cm^{-1}. The APZO hybrid particles show further vibrational bands at ~1149 and ~1019 cm^{-1}, which can be attributed to the vibrational modes of Si–O–Si groups formed by self-condensation of the organosilanes.

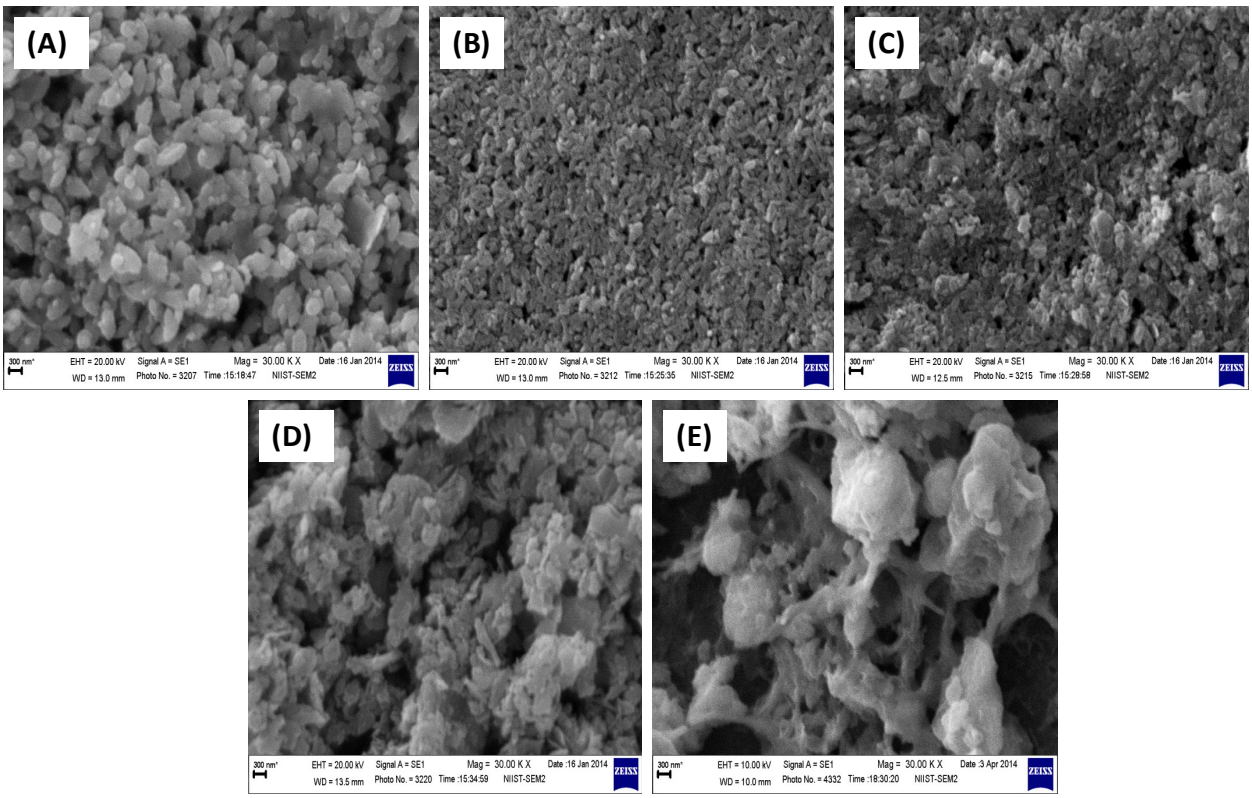

Fig. S2. SEM images of (A) 0, (B) 1, (C) 2, (D) 5, and (E) 20 mol.% APZO NHs. Scale bar 300 nm.

Morphological features. The SEM images of APZO NHs with various molar ratios were shown in Fig. S2. Upon increasing the concentration of APS, the morphology was also varied. The SEM images of without APS shows rice-like particle of ~ 300 nm in length can be seen in Fig. S2A. By increase in the amount of APS, the morphology was slightly changed due to the surface capping with APS. Since the effect of capping strongly influences the particle size reduction at the same scale bar confirmed from 1% APZO NHs morphology. Here, we noticed that the same rice-like morphology was obtained as in the case of 0% APZO NHs (Fig. S2B). As the concentration of APS increases, the hybrid morphology gradually changes to nanospherical. The aggregation tendency was increased due to the amorphous nature of silane capping which was covalently bonded to the ZnO surface to form a hybrid (Fig. S2C-E).

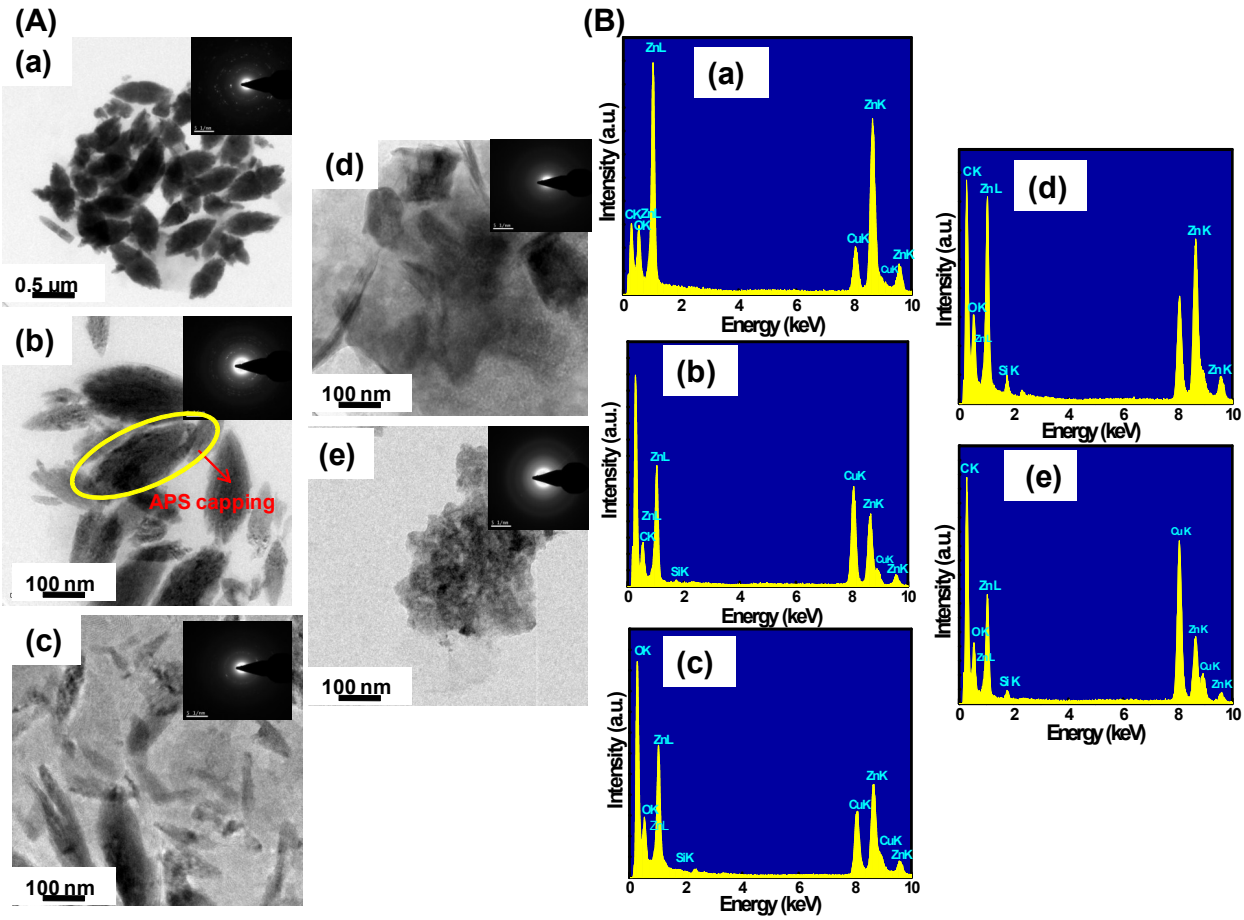

Fig. S3. TEM images of (A) (a) 0, (b) 1, (c) 2, (d) 5, and (e) 20% APZO NHs. The EDX spectra of the corresponding TEM images are shown in (B) (a), (b), (c), (d), and (e). The inset of the figures shows corresponding selected area electron diffraction (SAED) pattern.

Fig. S3A shows the TEM images of 0, 1, 2, 5 and 20% APZO NHs. The TEM images were observed to be same morphology as in SEM, which is further evidenced the actual morphology and size of synthesized samples. The 0% APZO NHs shows rice-like images in the scale bar 0.5µm (Fig. S3A(a)). The 1% APZO NHs clearly observed the surface coverage of APS with ZnO NPs (Fig. S3A(b)). The morphology of higher mol.% of APS evidenced the morphological changes (Fig. S3A(c)-(e)). The inset of the figures shows corresponding selected area electron

diffraction (SAED) pattern which can be indexed to the reflection of the monocrystalline wurtzite ZnO structure, and this is consistent with the XRD results. The chemical purity and elemental compositions of the APZO NHs were further detected by energy-dispersive X-ray (EDX) spectroscopy. In Fig. S3B depicted the corresponding EDX spectra of ZnO samples. In Fig. S3, except S3(a), reveals the presence Si which shows APS capped on the ZnO surface. It confirms that the APZO NHs was composed of the elements Zn, O, and Si.

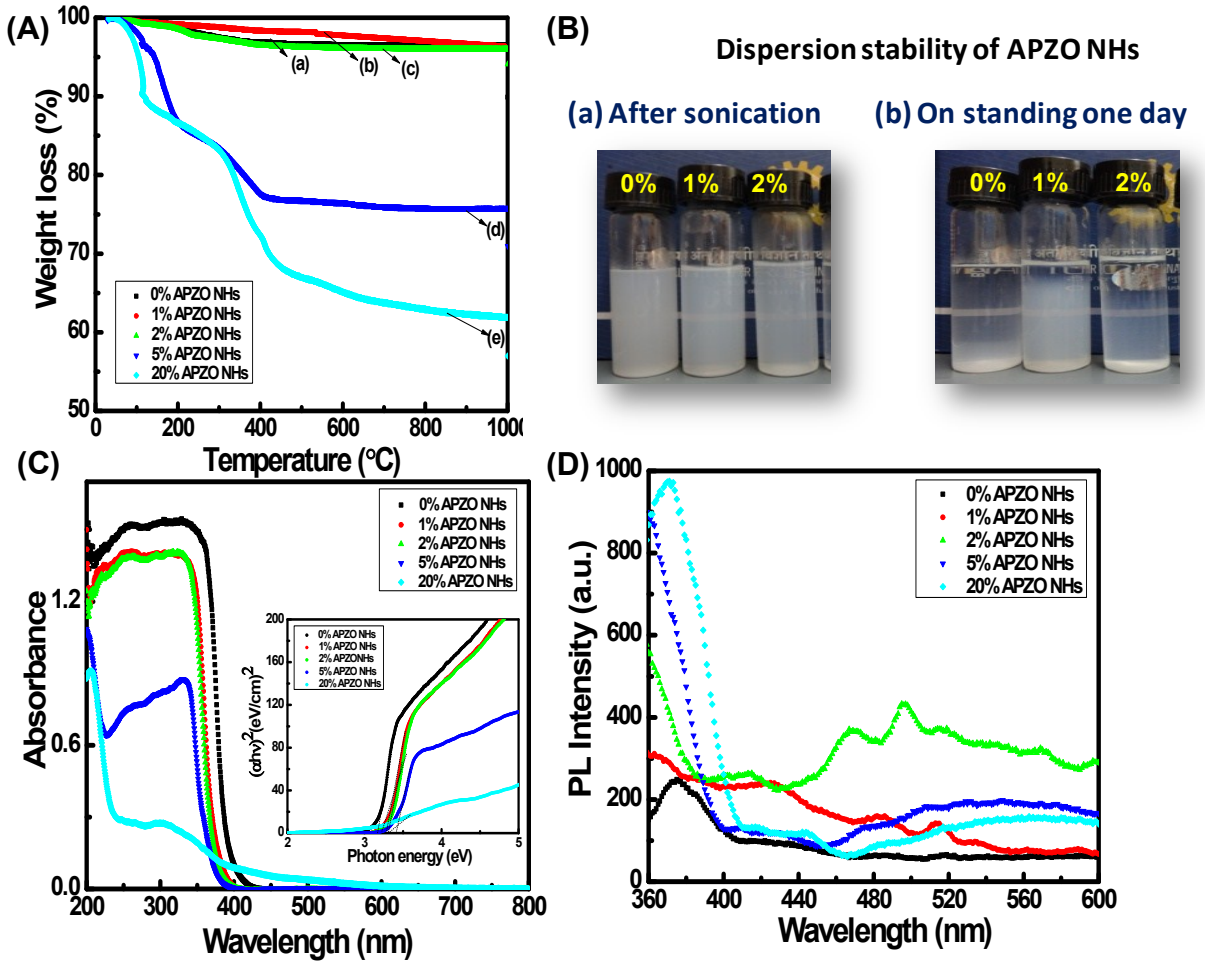

Fig. S4. (A) TG analysis of varying concentration APZO NHs. (B) Dispersion stability of 0.01 wt.% APZO NHs with different mol.% concentrations. (C) Solid-state UV-vis absorption spectra of APZO NHs. Inset shows evolution of the $(\alpha hv)^2$ *vs. hv* curves of respective samples. (D) PL spectra of different mol.% of APZO NHs.

Thermal properties. TG thermogram profiles taken for ZnO and silane modified hybrids nanoparticles are presented in Fig. S4A. In pure ZnO**,** two stage weight loss, the first one at temperature around 118 °C amounting to below 4 wt.% is estimated which is due to the removal of adsorbed water, and the second one centered at 400 °C assigned to the thermal decomposition of acetates ions bound to the ZnO surface is seen. In organo-modified samples, about 7% weight loss is seen at temperatures below 120 ^{o}C confirming the less amounts of adsorbed water molecules thus indicating a reduced hydrophilic character of ZnO samples containing surface organic species. Beside the weight loss at 100 °C, the TGA profiles of organo-modified ZnO samples show an additional weight loss with a maximum at 310 °C which can be assigned to the decomposition of the ammoniumpropyl groups. In the case of APS functionalized ZnO, at 310 °C the weight loss was increases gradually with respect to increasing mol.% of silane loading is due to decomposition of organic coating. The results of thermogravimetric analysis were used further to calculate the approximate grafting density of APS at the surface of ZnO. Considering loss due to the organic fragment, the grafting density was calculated using the expression, $Q^{TGA} = W/(M_{CF} \times S)$, where W= weight loss, M_{CF} = molecular weight of corresponding organic fragment, S=specific surface area of ZnO used. In Table S1, the morphology, crystallite size (<D>), particle diameter ($2r$), agglomeration coefficient (C_F), surface area (S_{BET}) and grafting density (Q^{TGA}) for the APZO NHs were determined and summarized. The photographic images (Fig. S4B) showed the colloidal stability of APZO NHs dispersed in water under ultrasonication for 15 min. and standing one day indicating that the 1% APZO NHs was colloidally stable in water medium.

Optical properties. Solid state UV-visible absorbance spectra of all samples, measured using $BaSO_4$ as reference, (Fig. S4C) showed a wide band in the 200–800 nm range with absorption

maxima at 362 nm for 0% APZO NHs. The absorption at 362 nm was assigned to the electronic transition from the valence band (mainly formed by orbitals of the oxide anions) to the conduction band (mainly formed by orbitals of the Zn^{2+} cations) of ZnO. The band gap for this transition was estimated to be 3.42 eV, slightly higher than the band gap typical of bulky ZnO samples (3.26 eV) and which were somehow more resolved for APZO NHs. The samples 1, 2, 5, and 20% APZO NHs shows absorption wavelength shows 343 (E_g=3.61 eV), 339 (E_g=3.66 eV), 334 (E_g=3.71 eV), and 316 (E_g= 3.92 eV) nm, respectively. By increasing the amount of organic moieties exposed on the ZnO surface, a blue-shift of the absorption band at lower wavelengths (passing from 360 nm to 340 nm) was observed. The blue-shift behavior or broadening in the band gap is mainly due to the Moss–Burstein band filling effect. Based on the Moss–Burstein theory, for the samples 1, 2, 5, and 20% APZO NHs, the donor electrons occupied states at the bottom of the conduction band. *Photoluminesence spectra:* The influence of the APS capping and surface functionalization on the inherent optical properties of APZO NHs, room temperature PL spectroscopy was performed on both the silane treated and untreated ZnO nanoparticle dispersion in water medium (Fig. S4D). The presence of the APS induces a stable, reproducible bimodal enhancement of the UV and visible emission intensity. The UV emission peak at ~375 nm in the pure ZnO NPs exhibit an intensity increases with increase in mol.% of APS. Compared to normal ZnO NPs, the APZO NHs shows the increase in intensity of visible emission peak at ~510 nm. The enhancement of UV emission occurs because it is the higher-energy process and therefore energeticaly less stable. A surfactant molecule with a relatively high local negative charge passivated the green emission due to the oxygen ions, during micelle formation, occupying vacancies on the positively charged nano-ZnO surface. This is not expected to occur within our APS capping approach where the APZO NHs is being synthesized in the bulk state.

As the APS surface coverage increases, the retention of the bimodal peak is anticipated. However, the relative intensities of UV and visible emission are expected to be influenced by the particle size distributions.

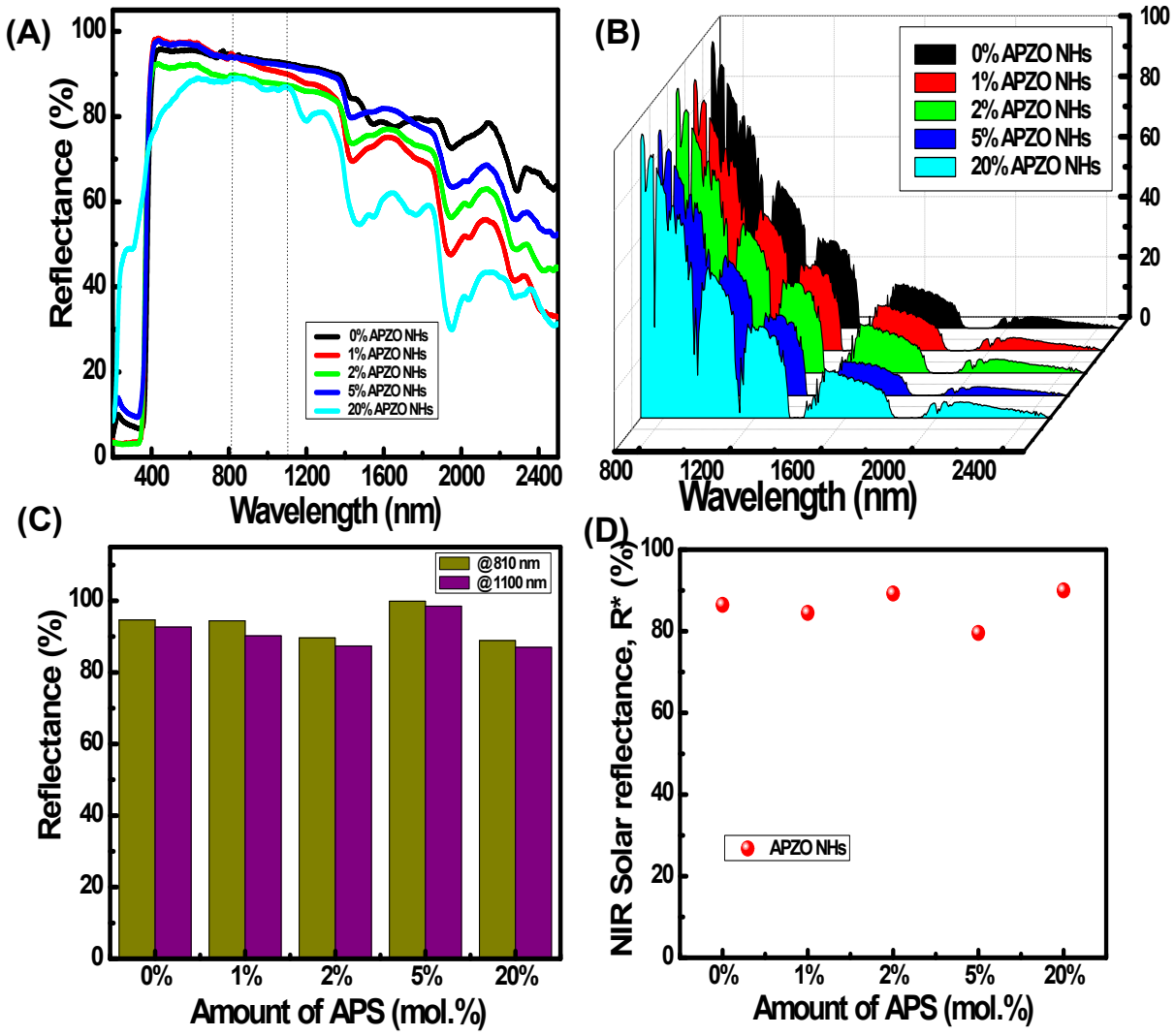

Fig. S5. (A) NIR reflectance of APZO NHs, (B) NIR solar reflectance spectra of APZO NHs, (C) Reflectance *vs.* APS concentration @ 810 and 1100 nm, (D) NIR Solar reflectance *vs.* amount of APS in mol.%.

NIR reflectance and NIR solar reflectance properties. NIR reflectance depends on the mean particle size coupled with smaller crystallite size. The NIR reflectance spectra of pure ZnO

NPs and APZO NHs are given in Figure S5A. Multiplying the (normalized) spectral irradiance of the Sun *i(λ)* by the spectral reflectivity yields the NIR solar reflectance spectrum presented in Fig. S5B. The NIR solar reflectance (R^*) of the 0, 1, 2, 5 and 20% APZO NHs are 86.45, 84.50, 89.26, 79.59 and 90.03%, respectively. Such the high NIR solar reflectance displayed by all the Zn/Si hybrids makes them as interesting candidates for use as cool white pigments. Table S2 illustrated the % NIR reflectance of APZO NHs @ 810 and 1100 nm wavelength and NIR solar reflectance of different mol.% of APZO NHs and its band gaps.

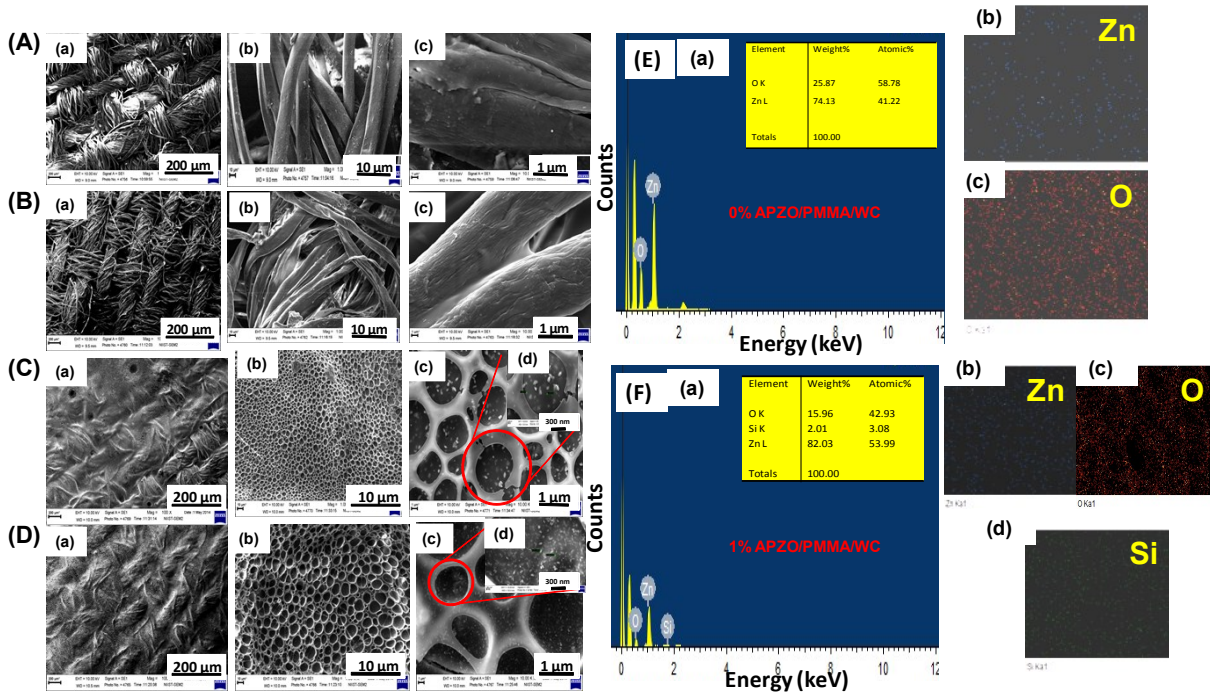

Fig. S6. SEM images of (A) bare WC, (B) PMMA/WC, (C) 0% APZO NHs/PMMA/WC-6 coatings and (D) 1% APZO NHs/PMMA/WC-6 coatings. The EDX patterns and its corresponding elemental mapping have reveals the elemental analysis of (E) 0% APZO NHs/PMMA/WC-6 coatings, and (F) 1% APZO NHs/PMMA/WC-6 coatings.

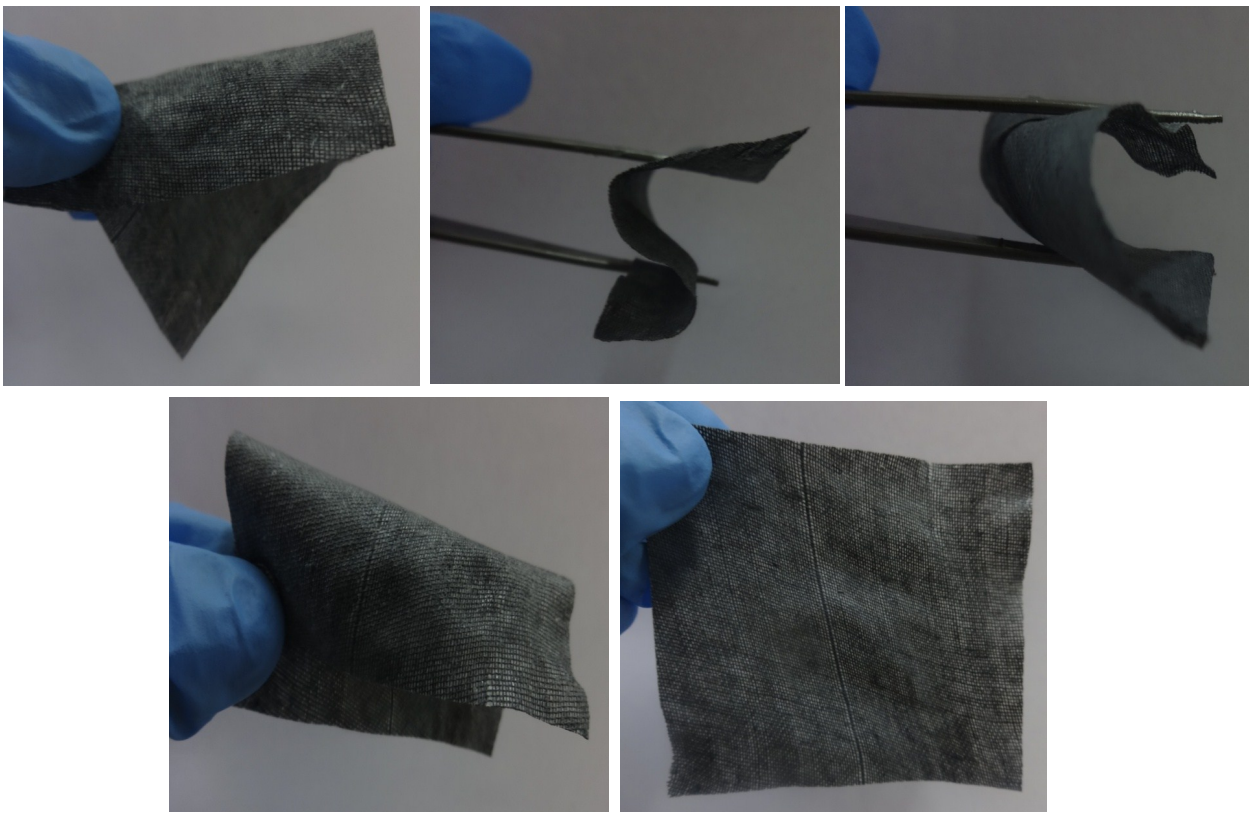

Fig. S7. A photograph of the cotton textile 1% APZO NHs/PMMA/BC coated with 7 layers.

Table S1. Morphology, DLS Particle Size, Zeta potential, Surface area determination of different mol.% of APZO NHs.

ZnO samples	**Morphology**	**[a]<D>** (nm)	**[b]ζ-Potential** (mV)	**[c]Z_{ave}** (nm)	**[d]2r** (nm)	**[e]S_{BET}** (m^2g^{-1})	**[f]Wt. loss from TGA (%)**	**[g][OH] ($mmolg^{-1}$)**	**[h]Q^{TGA}** ($\mu molm^{-2}$)
0% APZO	Macro-spindle	18.34	-52.2±8.80	337	4.7399	225.84	2.0079	2.2767	ND
1% APZO	Nano-spindle	18.56	-13.1±6.80	220	3.7333	286.73	0.7139	0.7989	13.98
2% APZO	Nano-spherical	21.16	7.46±5.44	239	3.5868	298.45	1.7757	2.0087	34.20
5% APZO	Nano-spherical	18.81	11.6±5.60	385	3.4227	312.76	12.766	16.260	228.0
20% APZO	Aggregated Spherical	Amorphous	-13.7±7.62	bimodal 255, 970	ND	ND	ND	ND	ND

[a]Crystallite size from XRD, [b] zeta potential, [c] particle size distribution analysis from DLS, [d]The particle size (radius) from effective mass modal using the equation: r (nm)=-0.3049+√(-26.23012+10240.72/λ_p)/(-6.3829+2483.2/λ_p), where r is the particle size (in radius), λ_p as peak

absorbance wavelength (λ_p) in nm for APZO NHs, [e]The BET specific surface area of nano-sized APZO powders can using the following equation: $S_{BET} = 6000/\rho d_{BET}$, where S_{BET} is the BET specific surface area (in m^2/g), ρ is the density of nanosized APZO powder and d_{BET} is the average crystalline size (in nm) from equation. From this study, S_{BET} was obtained by using the 5.605 g/cm^3 power density, [f]Recorded from 120 to 310 °C, at which the removal of the chemisorbed water occurs. [g]The hydroxyl group concentration was assessed according to [OH]= $2/M_{H2O}$ × [weight loss (%)/100-weight loss], where M_{H2O} is the molar mass of water and [h]grafting density. ND = not determined.

Table S2. NIR reflectance and NIR solar reflectance of different mol.% of APZO NHs and its band gaps are illustrated below:

Sample	**NIR Reflectance @ 810 nm**	**NIR Reflectance @ 1100 nm**	**NIR Solar reflectance, R***	**Absorption wavelength (nm)**	**Band gap (eV)**
Pure ZnO NPs	94.64	92.66	86.45	362	3.4248
1% APZO NHs	94.44	90.20	84.50	343	3.6146
2% APZO NHs	89.63	87.36	89.26	339	3.6572
5% APZO NHs	99.85	98.52	79.59	334	3.7119
20% APZO NHs	88.87	86.98	90.03	316	3.9234